

2009

# Preparation and characterization of protein-nanotube conjugates

Jonathan S. Dordick

Dhiral A. Shah

Ravindra C. Pangule

Shyam Sundhar Bale

Prashanth Asuri

Santa Clara University, [asurip@scu.edu](mailto:asurip@scu.edu)

*See next page for additional authors*

Follow this and additional works at: [https://scholarcommons.scu.edu/bio\\_eng](https://scholarcommons.scu.edu/bio_eng)

 Part of the [Biomedical Engineering and Bioengineering Commons](#)

---

## Recommended Citation

Shah, D.A., Pangule, R.C., Bale, S.S., Asuri, P., Joshi, A., Banerjee, A., ... Kane, R.S. (2009). Preparation and characterization of protein-nanotube conjugates. In *Methods in Bioengineering: Nanoscale Bioengineering and Nanomedicine* (pp. 1–23). Artech House.

Reproduced by permission from Kaushal Rege and Igor Medintz, *Methods in Bioengineering: Nanoscale Bioengineering and Nanomedicine*, Norwood, MA: Artech House, Inc., 2009. © 2009 by Artech House, Inc.

This Book Chapter is brought to you for free and open access by the School of Engineering at Scholar Commons. It has been accepted for inclusion in Bioengineering by an authorized administrator of Scholar Commons. For more information, please contact [rscroggin@scu.edu](mailto:rscroggin@scu.edu).

---

**Authors**

Jonathan S. Dordick, Dhiral A. Shah, Ravindra C. Pangule, Shyam Sundhar Bale, Prashanth Asuri, Amit Joshi, Akhilesh Banerjee, David Vance, and Ravi S. Kane

# Methods in Bioengineering

## Nanoscale Bioengineering and Nanomedicine

Kaushal Rege

Department of Chemical Engineering  
Arizona State University

Igor L. Medintz

Center for Biomolecular Science and Engineering  
U.S. Naval Research Laboratory

Editors



**ARTECH  
HOUSE**

BOSTON | LONDON  
[artechhouse.com](http://artechhouse.com)

**Library of Congress Cataloging-in-Publication Data**

A catalog record for this book is available from the U. S. Library of Congress.

**British Library Cataloguing in Publication Data**

A catalogue record for this book is available from the British Library.

ISBN-13: 978-1-59693-410-8

**Text design by Darrell Judd**

**Cover design by Igor Valdman**

© 2009 Artech House. All rights reserved.

Printed and bound in the United States of America. No part of this book may be reproduced or utilized in any form or by any means, electronic or mechanical, including photocopying, recording, or by any information storage and retrieval system, without permission in writing from the publisher.

All terms mentioned in this book that are known to be trademarks or service marks have been appropriately capitalized. Artech House cannot attest to the accuracy of this information. Use of a term in this book should not be regarded as affecting the validity of any trademark or service mark.

10 9 8 7 6 5 4 3 2 1

# Contents

Preface	xv
<b>CHAPTER 1</b>	
Preparation and Characterization of Carbon Nanotube-Protein Conjugates	1
1.1 Introduction	2
1.2 Materials	3
1.3 Methods	3
1.3.1 Physical Adsorption of Proteins on Carbon Nanotubes	3
1.3.2 Protein Assisted Solubilization of Carbon Nanotubes	4
1.3.3 Covalent Attachment of Proteins onto Carbon Nanotubes	5
1.4 Data Acquisition, Anticipated Results, and Interpretation of Data	7
1.4.1 Characterization of Proteins Physically Adsorbed onto Carbon Nanotubes	7
1.4.2 Characterization of Protein-Solubilized Carbon Nanotubes	11
1.4.3 Characterization of Covalently Attached Carbon Nanotube-Protein Conjugates	13
1.5 Discussion and Commentary	18
1.6 Applications Notes	19
1.7 Summary Points	21
Acknowledgments	21
References	21
<b>CHAPTER 2</b>	
Peptide-Nanoparticle Assemblies	25
2.1 Introduction	26
2.2 Materials	27
2.3 Methods	28
2.3.1 Coil-Coil Peptide Mediated NP Assembly	28
2.3.2 Synthesis of Hybrid Structures Using Multifunctional Peptides	31
2.4 Assembly Mediated by Metal Ion-Peptide Recognition	32
2.5 Peptides as Antibody Epitopes for Nanoparticle Assembly	33
2.6 DATA Acquisition, Anticipated Results, and Interpretation	34
2.7 Discussion and Commentary	35

2.8	Application Notes	36
2.9	Summary Points	36
	Acknowledgments	36
	References	37
<b>CHAPTER 3</b>		
	Nanoparticle-Enzyme Hybrids as Bioactive Materials	39
3.1	Introduction	40
3.2	Materials	40
3.3	Methods	41
3.3.1	Enzyme-Attached Polystyrene Nanoparticles	41
3.3.2	Polyacrylamide Hydrogel Nanoparticles for Entrapment of Enzymes	41
3.3.3	Magnetic Nanoparticles with Porous Silica Coating for Enzyme Attachment	42
3.3.4	Enzyme Loading and Activity Assay	42
3.4	Results	44
3.4.1	Polystyrene-Enzyme Hybrid Nanoparticles	44
3.4.2	Polyacrylamide Hydrogel Nanoparticles with Entrapped Enzymes	45
3.4.3	Magnetic Nanoparticles for Enzyme Attachment	46
3.5	Discussion and Commentary	47
3.6	Troubleshooting	49
3.7	Application Notes	49
3.8	Summary Points	49
	Acknowledgments	50
	References	50
<b>CHAPTER 4</b>		
	Self-Assembled QD-Protein Bioconjugates and Their Use in Fluorescence Resonance Energy Transfer	53
4.1	Introduction	54
4.2	Materials	56
4.2.1	Reagents	56
4.2.2	Equipment	56
4.3	Methods	56
4.3.1	Quantum Dot Synthesis	56
4.3.2	Surface Ligand Exchange	58
4.3.3	Biomolecule Conjugation	61
4.3.4	Fluorescence Measurements	65
4.4	Data Analysis and Interpretation	66
4.4.1	Calculating Donor-Acceptor Distances	68
4.4.2	Calculating Reaction Rates of Surface-Bound Substrates	70

4.5	Summary Points	72
4.6	Conclusions	72
	References	72
	Annotated References	74
<b>CHAPTER 5</b>		
	Tracking Single Biomolecules in Live Cells Using Quantum Dot Nanoparticles	75
5.1	Introduction	76
5.2	Materials	78
	5.2.1 Reagents	78
	5.2.2 Imaging Equipment	79
5.3	Methods	79
	5.3.1 Forming QD Bioconjugates	79
	5.3.2 Treating Cells with QD Bioconjugates	79
5.4	Data Acquisition, Anticipated Results, and Interpretation	79
	5.4.1 Imaging QD-Bound Complexes in Cells	79
	5.4.2 Analysis of the Real-Time QD Dynamics	80
5.5	Discussion and Commentary	81
	References	82
<b>CHAPTER 6</b>		
	Nanoparticles as Biodynamic Substrates for Engineering Cell Fates	85
6.1	Introduction	86
6.2	Experimental Design	88
6.3	Materials	88
	6.3.1 Cell Culture, Fixing, Staining, and Analysis Reagents	88
	6.3.2 Nanoparticle Fabrication and Functionalization	89
	6.3.3 Microscale Plasma Initiated Patterning	89
6.4	Methods	89
	6.4.1 Albumin Nanoparticle Fabrication	89
	6.4.2 Albumin Nanoparticle Functionalization	91
	6.4.3 Albumin Nanoparticle Pattern Creation—Microscale Plasma Initiated Patterning ( $\mu$ PIP)	93
	6.4.4 Cell Culture	94
	6.4.5 Keratinocyte Morphology and Migration	94
	6.4.6 Fibroblast Extracellular Matrix Assembly	94
	6.4.7 Cell Attachment Assay	95
6.5	Results	95
	6.5.1 Enhanced Cell Migration	95
	6.5.2 Enhanced Extracellular Matrix Assembly	97
6.6	Discussion of Pitfalls	100
	6.6.1 Spatial Guidance of Cell Attachment—Microscale Plasma Initiated Patterning	100

6.6.2	Three-Dimensional Presentation of Albumin Nanoparticles	101
6.7	Summary Points	102
	Acknowledgments	103
	References	103
<b>CHAPTER 7</b>		
	Magnetic Cell Separation to Enrich for Rare Cells	107
7.1	Introduction	108
7.1.1	Principle	110
7.1.2	Examples of Cell Magnetic Separation Applications	115
7.2	Materials and Methods	116
7.2.1	Enrichment Process	116
7.2.2	Red Cell Lysis Step	117
7.2.3	Immunomagnetic Labeling	117
7.2.4	Magnetic Cell Separation Step	117
7.3	Data Acquisition, Results, and Interpretation	117
7.4	Discussion and Commentary	120
7.5	Summary Points to Obtain High-Performance, Magnetic Cell Separations	120
	Acknowledgments	120
	References	121
<b>CHAPTER 8</b>		
	Magnetic Nanoparticles for Drug Delivery	123
8.1	Introduction	124
8.2	Experimental Design	124
8.3	Materials	126
8.3.1	Reagents	126
8.3.2	Facilities and Equipment	127
8.4	Methods	128
8.4.1	Synthesis of Magnetic Nanoparticles	128
8.4.2	Physical Characterization of Magnetic Nanoparticles	129
8.4.3	Conversion of DOX•HCl	129
8.4.4	Drug Loading and Release Kinetics	129
8.4.5	Kinetics of DOX Release from Magnetic Nanoparticles	130
8.4.6	Antiproliferative Activity of Doxorubicin Loaded Magnetic Nanoparticles on MCF-7 Cells	131
8.4.7	Antiproliferative Activity of Doxorubicin Loaded Magnetic Nanoparticles on MCF-7 Cells in the Presence of a Magnetic Field	131
8.5	Data Acquisition, Anticipated Results, and Interpretation	132
8.6	Discussion and Commentary	133
8.7	Application Notes	134



8.8 Summary Points	134
Acknowledgments	135
References	135

## CHAPTER 9

Imaging and Therapy of Atherosclerotic Lesions with Theranostic Nanoparticles	137
9.1 Introduction	138
9.2 Experimental Design	139
9.3 Materials	140
9.3.1 Reagents	140
9.3.2 Facilities/Equipment	140
9.3.3 Animal Model	141
9.3.4 Alternate Reagents and Equipment	141
9.4 Methods	141
9.4.1 Synthesis of Theranostic Nanoparticles	141
9.4.2 Intravital Fluorescence Microscopy	143
9.4.3 Light-Based Therapy	144
9.5 Data Acquisition, Anticipated Results, and Interpretation	145
9.5.1 Characterization of Theranostic Nanoparticles	145
9.5.2 Animal Experimentation	146
9.5.3 Intravital Fluorescence Microscopy	146
9.5.4 Statistical Analyses	147
9.5.5 Anticipated Results	148
9.6 Discussion and Commentary	148
9.7 Summary Points	149
Acknowledgments	150
References	150

## CHAPTER 10

Biomedical Applications of Metal Nanoshells	153
10.1 Introduction	154
10.1.1 Biomedical Applications of Metal Nanoshells	154
10.1.2 Nanoshells for Combined Optical Contrast and Therapeutic Application	155
10.2 Experimental Design	156
10.3 Materials	156
10.3.1 Nanoparticle Production	156
10.3.2 Protein Conjugation to Nanoshells Surface	156
10.3.3 Cell Culture	157
10.3.4 In Vitro Assays	157
10.4 Methods	157
10.4.1 Fabrication of Gold/Silica Core Nanoshells	157
10.4.2 Nanoshells for Combined Imaging and Therapy In Vivo	158

10.4.3	Passivation of Nanoshells with PEG	159
10.4.4	Conjugation of Biomolecules to Nanoshells	160
10.4.5	Quantification of Antibodies on Nanoshells	160
10.5	Results	161
10.5.1	Gold/Silica Nanoshells Allow Both Imaging Contrast Increase and Therapeutic Benefit	161
10.5.2	Evaluation of Antibody Concentration per Nanoshell	163
10.6	Discussion of Pitfalls	163
10.7	Statistical Analysis	165
	Acknowledgments	166
	References	166

## CHAPTER 11

	Environmentally Responsive Multifunctional Liposomes	169
11.1	Introduction	170
11.1.1	Cis-Aconityl Linkage	171
11.1.2	Trityl Linkage	172
11.1.3	Acetal Linkage	172
11.1.4	Polyketal Linkage	172
11.1.5	Vinyl Ether Linkage	172
11.1.6	Hydrazone Linkage	173
11.1.7	Poly(Ortho-Esters)	173
11.1.8	Thiopropionates	173
11.2	Materials	174
11.2.1	Chemicals	174
11.2.2	Syntheses	175
11.2.3	Preparation of the TATp-Bearing, Rhodamine-Labeled Liposomal Formulations	175
11.2.4	Preparation of the TATp-Bearing, Rhodamine Labeled, pGFP Complexed Liposomal Formulations	175
11.3	Methods	176
11.3.1	Synthesis of Hydrazone-Based mPEG-HZ-PE Conjugates	176
11.3.2	Synthesis of PE-PEG <sub>1000</sub> -TATp Conjugate	183
11.3.3	In Vitro pH-Dependant Degradation of PEG-HZ-PE Conjugates	184
11.3.4	Avidin-Biotin Affinity Chromatography	184
11.3.5	In Vitro Cell-Culture Study	184
11.3.6	In Vivo Study	185
11.3.7	In Vivo Transfection with pGFP	185
11.4	Discussion and Commentary	185
11.4.1	Synthesis of Hydrazone-Based mPEG-HZ-PE Conjugates	185
11.4.2	Synthesis of PE-PEG <sub>1000</sub> -TATp Conjugate	186
11.4.3	In Vitro pH-Dependant Degradation of PEG-HZ-PE Conjugates	186

11.4.4	Avidin-Biotin Affinity Chromatography	188
11.4.5	In Vitro Cell Culture Study	188
11.4.6	In Vivo Study	188
11.4.7	In Vivo pGFP Transfection Experiment	189
11.5	Conclusion	191
11.7	Summary Points	192
	Acknowledgments	192
	References	192

## CHAPTER 12

	Biodegradable, Targeted Polymeric Nanoparticle Drug Delivery Formulation for Cancer Therapy	197
12.1	Introduction	198
12.2	Materials	200
12.2.1	Polymer Synthesis of PLA-PEG and PLGA-PEG	200
12.2.2	Nanoparticle Formation	201
12.2.3	Ligand Conjugation	201
12.2.4	Quantification of Drug Encapsulation	201
12.2.5	Release Experiments	202
12.2.6	Postformulation Treatment	202
12.2.7	Cell Binding and Uptake Experiments	202
12.2.8	Cytotoxicity Experiments	203
12.3	Methods	203
12.3.1	Polymer Synthesis of PLA-PEG and PLGA-PEG	204
12.3.2	Nanoparticle Formation	207
12.3.3	Conjugation of Targeting Ligand	209
12.3.4	Quantification of Drug Encapsulation	211
12.3.5	Drug Release Studies	212
12.3.6	Postformulation Treatment	213
12.3.7	In Vitro Experiments: Cell Binding and Uptake Studies	214
12.3.8	In Vitro Experiments: Cytotoxicity Studies	215
12.4	Data Acquisition, Results, and Interpretation	216
12.4.1	Polymer Characterization	216
12.4.2	Nanoparticle characterization	217
12.4.3	In Vitro Experiments	220
12.5	Discussion and Commentary	222
12.5.1	Particle Size	222
12.5.2	Particle Shape	224
12.5.3	Surface Chemistry	224
12.5.4	Drug Loading	225
12.5.5	Drug Release	226
12.5.6	Active Targeting and Ligand Conjugation	228
12.6	Troubleshooting Tips	230

12.7	Application Notes	230
12.8	Summary Points	231
	Acknowledgments	231
	References	231

## CHAPTER 13

	Porous Silicon Particles for Multistage Delivery	237
13.1	Introduction	238
13.2	Fabrication of PSPs	245
	13.2.1 Materials	245
	13.2.2 Methods	247
	13.2.3 Characterization	251
13.3	Oxidation and Surface Modification with APTES of PSPs	252
	13.3.1 Reagents	252
	13.3.2 Methods	252
13.4	Fluorescent Dye Conjugation of PSPs	254
	13.4.1 Reagents	254
	13.4.2 Methodology	254
13.5	Zeta Potential Measurement	254
	13.5.1 Equipment	254
	13.5.2 Reagents	254
	13.5.3 Methodology	254
	13.5.4 Results	255
13.6	Count and Size Analysis of PSPs	255
	13.6.1 Materials	255
	13.6.2 Methods	255
	13.6.3 Data Acquisition, Anticipated Results, and Interpretation	256
13.7	Using Inductively Coupled Plasma–Atomic Emission Spectroscopy (ICP–AES) to Determine the Amount of Degraded Silicon in Solution	257
	13.7.1 Materials	257
	13.7.2 Methods	258
	13.7.3 Data Acquisition, Anticipated Results, and Interpretation	258
13.8	Flow Cytometry to Characterize PSP Shape, Size, and Fluorescence Intensity	260
	13.8.1 Materials	262
	13.8.2 Methods	262
	13.8.3 Data Acquisition, Anticipated Results, and Interpretation	263
13.9	Loading and Release of Second-Stage NPs from PSPs	264
	13.9.1 Loading of NP into PSPs	264
	13.9.2 Release of NPs from PSPs	265
	13.9.3 Data Acquisition, Anticipated Results, and Interpretation	265
13.10	Discussion and Commentary	267
	Acknowledgments	271

References	271
<b>CHAPTER 14</b>	
Mathematical Modeling of Nanoparticle Targeting	275
14.1 Introduction	276
14.2 Molecular/Cellular Scale	277
14.2.1 Methods	277
14.2.2 Data Acquisition, Anticipated Results, and Interpretation	280
14.2.3 Discussion and Commentary	280
14.3 Tissue Scale	282
14.3.1 Methods	282
14.3.2 Data Acquisition, Anticipated Results, and Interpretation	284
14.3.3 Discussion and Commentary	284
14.4 Organism Scale	285
14.4.1 Methods	285
14.4.2 Data Acquisition, Anticipated Results, and Interpretation	286
14.4.3 Discussion and Commentary	287
14.5 Model Validation and Application	287
14.5.1 Statistical Guidelines	287
14.6 Summary Points	289
Acknowledgments	290
References	290
<b>CHAPTER 15</b>	
Techniques for the Characterization of Nanoparticle-Bioconjugates	293
15.1 Introduction	294
15.2 Methods	296
15.2.1 Separation-Based Techniques	296
15.2.2 Scattering Techniques	300
15.2.3 Microscopy	308
15.2.4 Spectroscopic	312
15.2.5 Mass Spectroscopy	317
15.2.6 Thermal Techniques	318
15.3 Summary Points	319
Acknowledgments	320
References	321
About the Editors	333
List of Contributors	334
Index	337

# Preparation and Characterization of Carbon Nanotube-Protein Conjugates

Jonathan S. Dordick,\* Dhiral A. Shah, Ravindra C. Pangule, Shyam Sundhar Bale, Prashanth Asuri, Amit Joshi, Akhilesh Banerjee, David Vance, and Ravi S. Kane\*

Department of Chemical and Biological Engineering, Rensselaer Polytechnic Institute, Troy, NY

\*Corresponding Authors: Prof. Ravi S. Kane, Department of Chemical and Biological Engineering, Rensselaer Polytechnic Institute, 110 8th Street, Troy, NY 12180, Phone: 518-276-2536, Fax: 518-276-4030, e-mail: kaner@rpi.edu; Prof. Jonathan S. Dordick, Department of Chemical and Biological Engineering, Rensselaer Polytechnic Institute, 110 8th Street, Troy, NY 12180, Phone: 518-276-2899, Fax: 518-276-2207, e-mail: dordick@rpi.edu

## Abstract

This chapter describes methods of immobilizing proteins on carbon nanotubes, using two different routes—physical adsorption and covalent attachment. We also provide an overview on how such conjugates can be characterized with the help of various techniques, such as Raman, Fourier transform infrared (FT-IR), circular dichroism (CD), and fluorescence spectroscopies, in addition to the standard enzyme kinetic analyses of activity and stability. Both the attachment routes—covalent and noncovalent—could be used to prepare protein conjugates that retained a significant fraction of their native structure and function; furthermore, the protein conjugates were operationally stable, reusable, and functional even under harsh denaturing conditions. These studies therefore corroborate the use of these immobilization methods to engineer functional carbon nanotube-protein hybrids that are highly active and stable.

### Key terms

enzyme immobilization  
carbon nanotubes  
physical adsorption  
covalent attachment  
nanotube solubilization

## 1.1 Introduction

Nanomaterials, such as carbon nanotubes (CNTs) offer a unique combination of electrical, mechanical, thermal, and optical properties [1] that make them promising materials for various applications ranging from sensing [2] and diagnostics to biotransformations and the cellular delivery of peptides and proteins [3, 4]. For instance, Barone et al. [5] have developed carbon nanotube-glucose oxidase conjugates that can act as glucose sensors. Recently, Dai and coworkers [2] demonstrated the recognition of monoclonal antibodies by a recombinant human antigen immobilized onto carbon nanotubes. Carbon nanotubes have also been used for both biomolecule delivery and targeted therapy. Pantarotto et al. [3] demonstrated that carbon nanotubes functionalized with peptides can penetrate cell membranes of human and murine fibroblasts, and serve as carriers for biomolecule delivery. Dai and coworkers [4] observed internalization of nanotube-protein conjugates in nonadherent human cancer cells as well as adherent cell lines. Kam et al. [6] demonstrated that functionalized CNTs could be used to selectively target cancer cells and destroy them by irradiating CNTs with near-infrared (NIR) light. These studies represent a fraction of the exciting opportunities at the interface of nanotechnology and biotechnology. It is, however, important to interface carbon nanotubes with biomolecules, such as proteins, to realize some of these applications. As a result, various methods of functionalization have been developed recently to functionalize CNTs with proteins. In this chapter, we describe three methods of preparing carbon nanotube-protein conjugates, each of them possessing distinct structural, mechanical, and functional characteristics.

Noncovalent attachment is probably the simplest technique for attaching proteins onto carbon nanotubes. The adsorption of proteins onto CNTs is hypothesized to be a result of the attractive hydrophobic interactions between carbon nanotubes and proteins [7]. This method has been found to preserve a significant fraction of the native structural and functional properties of several proteins as well as the physicochemical properties of nanotubes [2, 8–10]. The resulting formulations prevail in the form of aggregates, which can be easily separated from other solution components. However, the limited solubility of these conjugates in water limits their attractiveness for many applications in biotechnology [11, 12]. Nevertheless, such conjugates have been used for biosensing, diagnostics and preparing antifouling nanocomposites films [13].

To overcome the aforementioned limitation of water solubility, Karajanagi et al. have described a simple method that uses proteins to solubilize single-walled carbon nanotubes (SWNTs) in water [14]. Efficient solubilization of SWNTs has previously been achieved using surfactants [15, 16], polymers [17, 18], single stranded DNA [19], peptides [20], and polysaccharides [12, 21]. The direct solubilization of SWNTs using a variety of proteins differing in size and structure is a simple and scalable alternative that enables the generation of individual nanotube solutions. Moreover, proteins are rich in structure and function and have numerous reactive groups, such as hydroxyls, amines, thiols, carboxylic acids, and others, which can be used as orthogonal reactive handles for further functionalization of SWNTs.

Finally, Asuri et al. have developed an alternative method of preparing water-soluble conjugates of carbon nanotubes with a broad range of proteins [22]. CNTs can be acid oxidized to produce hydrophilic carboxylic acid and hydroxyl groups along their side-walls [23, 24], thereby leading to water solubility. Proteins can then be covalently attached to oxidized water-soluble CNTs using carbodiimide activation of the carboxylic

acid groups. These water-soluble conjugates not only display low diffusional resistance [25] and high activity with stable protein attachment [26], but also have added advantages of high stability and reusability, thereby overcoming the traditional limitations of water-soluble proteins. Though the covalent immobilization of proteins onto CNTs leads to stable protein attachment, the chemical modification of the CNTs surface may compromise the desirable electronic properties of CNTs. Such water-soluble CNT-protein conjugates may find application in fields other than biosensing, for example, biotransformations, biomaterials, medicine, and self-assembled materials.

It is, therefore, clear that many methods have been explored to prepare functional nanotube-protein conjugates. Each of these methods possesses its own unique set of advantages and disadvantages, and the best choice of the method depends on the desired end application of the hybrid conjugates.

## 1.2 Materials

Raw and purified HiPCO single-walled carbon nanotubes (SWNTs) (1–1.5 nm diameter, ca. 10  $\mu\text{m}$  length, <35 wt% ash content) were purchased from Unidym (Houston, TX). Multiwalled carbon nanotubes (MWNTs) (10–20 nm diameter, 5–20  $\mu\text{m}$  length, 95 wt% purity) were purchased from Nanolab, Inc. (Newton, MA). Enzymes—soybean peroxidase (SBP), horseradish peroxidase (HRP) and *Mucor javanicus* lipase (MJL)—were purchased from Sigma-Aldrich (St. Louis, MO) as salt-free, dry powders. Bicinchoninic acid (BCA) assay kit for determining solution phase protein concentrations was purchased from Pierce Biotechnology, Inc. (Rockford, IL). Guanidine hydrochloride (GdnHCl), sodium dodecylbenzene sulfonate (NaDDBS), and all other chemicals were obtained from Sigma. Bovine serum albumin (BSA) was purchased from Fisher Scientific International, Inc. (Hampton, NH). All other chemicals were obtained from Sigma-Aldrich (St. Louis, MO). All enzymes and chemicals were used as received without any further purification.

## 1.3 Methods

### 1.3.1 Physical Adsorption of Proteins on Carbon Nanotubes

Attachment of proteins to carbon nanotubes via physical adsorption represents a facile method of preparing nanotube-protein conjugates, wherein an aqueous dispersion of SWNTs is mixed with a protein solution to achieve adsorption. The unadsorbed protein is washed off and nanotube-protein conjugates are then resuspended in aqueous solution. The detailed procedure is described below:

1. Sonicate a fixed amount of raw SWNTs in dimethylformamide (DMF) at a concentration of 1 mg/mL for 30 minutes using a bath sonicator (Model 50T, VWR International, West Chester, PA) with rated power of 45W to obtain a uniform dispersion in solution.
2. Dispense 1 mL of the resulting SWNT dispersion into an Eppendorf microcentrifuge tube, and centrifuge the solution at 8,000 rpm for 1 minute. Remove the supernatant and resuspend the settled SWNTs in an aqueous buffer (50 mM phosphate buffer, pH



7.0) by vortexing the solution. Repeat this wash procedure at least five more times to remove any residual organic solvent. This gradual change from organic phase to an aqueous phase renders unfunctionalized SWNTs more dispersed in buffer. Finally, disperse 1 mg SWNTs in 500  $\mu\text{L}$  aqueous buffer (15 minutes).

NOTE: The selection of buffer for preparing conjugates is dependent upon the choice of protein and the retention of its native function in that buffer.

3. Prepare a fresh solution of protein in the aqueous buffer. Add the aqueous dispersion of SWNTs (500  $\mu\text{L}$ , 2 mg/mL) to the protein solution (500  $\mu\text{L}$ ), and shake the mixture on a platform shaker for 2 hours at 200 rpm and room temperature (2 hours 15 minutes).

NOTE: In the case of thermally unstable proteins or enzymes undergoing autolysis, such as trypsin, shaking should be carried out at 4°C to prevent deactivation during incubation.

4. After incubation, centrifuge the SWNT dispersion at about 8,000 rpm for 1 minute to settle the SWNT-protein conjugates. Carefully decant the supernatant (ca. 800  $\mu\text{L}$ ) without loss of any conjugates. Typically, perform six such washes, with fresh buffer added each time to remove unbound protein (20 minutes).

NOTE: While collecting the supernatant, tilt the microcentrifuge tube and gently pipette out approximately 800  $\mu\text{L}$  supernatant from close to the tube walls without disturbing the settled SWNTs, so that the supernatant does not contain SWNTs, which can interfere with BCA assay for protein content determination in supernatants. A swinging bucket microcentrifuge is ideal for this step, as the SWNTs settle at the bottom and not on the walls of the tube after centrifugation. Do not resuspend the SWNT-protein conjugates by vortexing, as this can lead to desorption of the protein from SWNT surface. Resuspend the conjugates by gently inverting and tapping the microcentrifuge tube containing the conjugates.

5. Analyze the supernatants for protein content using the BCA assay (for protein concentration range of 20–2,000  $\mu\text{g}/\text{mL}$ ) or the micro-BCA assay (for protein concentration range of 0.5–20  $\mu\text{g}/\text{mL}$ ). Determine the amount of protein attached onto the SWNTs by mass balance. Use the SWNT-protein dispersion for further analysis and characterization. (1 hour 15 minutes) The process flowchart is shown in Figure 1.1.

The total time to carry out the procedure is approximately 5 hours.

### 1.3.2 Protein Assisted Solubilization of Carbon Nanotubes

For preparation of protein solubilized carbon nanotubes, an aqueous dispersion of nanotubes is dispensed in a concentrated protein solution and exposed to ultrasonication for a predetermined time period. The supernatant, collected after sequential steps of ultracentrifugation of the CNT-protein dispersion, contain solubilized carbon nanotubes that are stable at room temperature and show no signs of aggregation. The detailed procedure is described below:

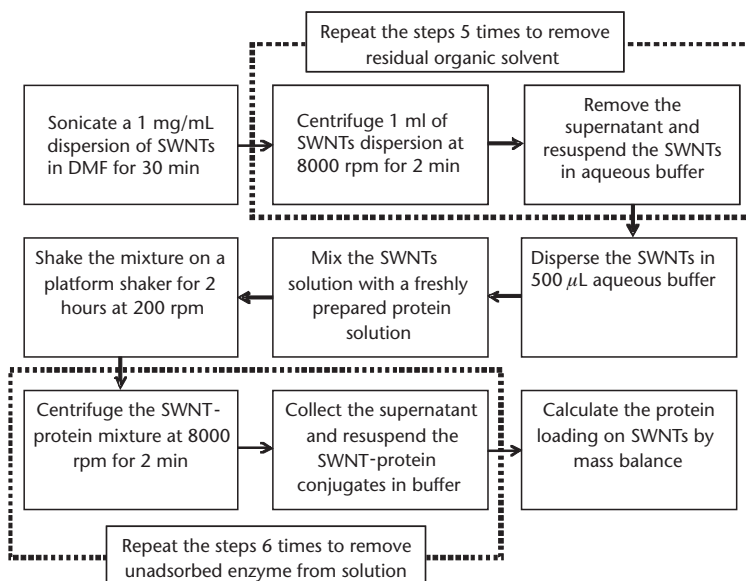


**Figure 1.1** Process flowchart for the physical adsorption of proteins onto SWNTs.

1. Disperse purified SWNTs in DMF at a concentration of 1 mg/mL by sonication, and replace the organic phase gradually with an aqueous phase through repeated washing with milliQ water (as stated in section 1.3.1) (45 minutes).
2. Disperse 200  $\mu\text{g}$  of SWNTs in 4-mL protein solution (10 mg/mL) and sonicate the dispersion of SWNTs for 2 hours using a bath sonicator (Model 50T, VWR International, West Chester, PA) with rated power of 45W (2 hours).
3. Ultracentrifuge the dispersed solution at 123,000g for 30 minutes.
4. Carefully collect 60% of the supernatant and ultracentrifuge at 185,000g for 30 minutes.
5. Collect 75% of the supernatant that contains protein adsorbed SWNTs. Use this solution for further analysis and characterization.

The total time to carry out the procedure is approximately 4 hours.

NOTE: The sonication efficiency and, hence, the quality of the dispersion varies with the volume of the solution sonicated. For best dispersions, use 4 mL volume for sonication.

### 1.3.3 Covalent Attachment of Proteins onto Carbon Nanotubes

For covalently attaching proteins onto carbon nanotubes, the carbon nanotubes are first functionalized with carboxylic acid groups by acid treatment. The carboxylic acid groups are then “activated” to form succinimide esters using carbodiimide chemistry [23]. These activated carboxylic groups react with amine groups on proteins enabling the covalent attachment of proteins onto carbon nanotubes. A detailed description of the procedure is given below:

1. Sonicate a fixed amount of multiwalled carbon nanotubes (MWNTs) in a mixture of concentrated sulfuric acid and nitric acid (3:1, v/v; 400 mL/100 mg carbon nanotubes) using a bath sonicator with a rated power of 45W for 3 hours. Periodically replace the contents of the bath with ice cold water to ensure that the MWNT suspension does not get heated up during sonication (3 hours).

NOTE: Acid oxidation not only leads to the functionalization of MWNTs with carboxylic acid groups, but also causes cutting of MWNTs. Longer sonication times result in finer oxidized MWNTs.

2. Add the nanotube-containing acid solution (400 mL) to an ice-cold solution of milliQ water (3,600 mL) gradually with constant swirling. Allow 10 to 15 minutes for dissipation of the heat generated on diluting the acid mixture.
3. Filter the solution through a 0.22- $\mu$ m polycarbonate filter membrane (Isopore membrane, Millipore) in batches of approximately 200 mL to remove the acid. After each filtration, disperse the nanotube film or bucky paper (a mass of carbon nanotubes tangled with each other to form a film or mat) thus formed in 50-mL milliQ water by ultrasonication in the bath sonicator for approximately 10 minutes, until the nanotubes are dispersed entirely in solution. Dilute this suspension with 150-mL milliQ water (40 minutes).
4. Repeat the ultrasonication/filtration step at least three times until water-soluble MWNTs are obtained and the pH of the filtrate becomes neutral (2 hours).

NOTE: These oxidized and “cut” nanotubes can be stored in aqueous solution (1 mg/mL) at room temperature.

5. After the final filtration, disperse the oxidized nanotubes (2 mg/mL) in MES (2-(*N*-Morpholino) ethanesulfonic acid) buffer (50 mM, pH 6.2), and add an equal volume of 400-mM *N*-hydroxysuccinimide (NHS) in MES buffer (5 minutes).
6. Sonicate the mixture for 30 minutes in a bath sonicator.
7. Add *N*-ethyl-*N'*-(3-dimethylaminopropyl) carbodiimide hydrochloride (EDC) (20 mM in MES buffer) to the nanotube solution to initiate the coupling of NHS to the carboxylic groups on the oxidized nanotubes, and stir the mixture at 400 rpm for 30 minutes at room temperature.
8. Filter the activated nanotube solution through a polycarbonate filter membrane (0.22  $\mu$ m) and rinse thoroughly with MES buffer to remove excess EDC and NHS (20 minutes).
9. Transfer the nanotube film immediately into a freshly prepared protein solution (2 mg/mL, 10 mM phosphate buffer, pH 8.0), and sonicate for few seconds to disperse the nanotubes in solution.

NOTE: Do not allow the nanotube film to dry out completely on the filter membrane as it may lead to hydrolysis of the active ester and hence decreased attachment of the protein.

10. Shake the mixture on an orbital shaker at 200 rpm for 3 hours and at room temperature to allow the attachment of proteins to the nanotubes.

NOTE: Proteins such as proteases or thermally unstable proteins require that this step be carried out at 4°C to prevent protein deactivation.

11. Filter the nanotube-protein suspension and wash it three times with milliQ water (5-mL/mg nanotubes) and once with 1% Tween-20 (5-mL/mg nanotube) to remove any nonspecifically bound protein (2 hours).
12. Allow flocculates of nanotube-protein conjugates, if any, to settle overnight and use the supernatant for further experiments.
13. Quantify the amount of immobilized protein by elemental analysis of the oxidized nanotubes and the nanotube-protein conjugates. The schematic of the process of protein functionalization on nanotubes is shown in Figure 1.2.

The total time to carry out the procedure is approximately 11 hours.

## 1.4 Data Acquisition, Anticipated Results, and Interpretation of Data

We have employed various techniques, such as Raman, FT-IR, CD, and fluorescence spectroscopies in addition to the standard enzyme kinetic analyses of activity and stability, to understand how the attachment onto CNTs influences protein structure and function. The choice of technique depends on the method used for protein attachment and the resulting characteristics of the formulation (e.g., protein loading and dispersibility). In this section, we discuss these characterization techniques and include our own data of experiments to enable the reader to evaluate the CNT-protein conjugates prepared by the previously described methods of protein attachment onto carbon nanotubes.

### 1.4.1 Characterization of Proteins Physically Adsorbed onto Carbon Nanotubes

We have used enzymes as probes of protein structure and function. To measure the retention of enzyme activity upon attachment, it is necessary to quantify the amount of enzyme physically adsorbed onto carbon nanotubes. Measuring enzyme activity and detecting the change in its secondary structure by FT-IR spectroscopy before and after

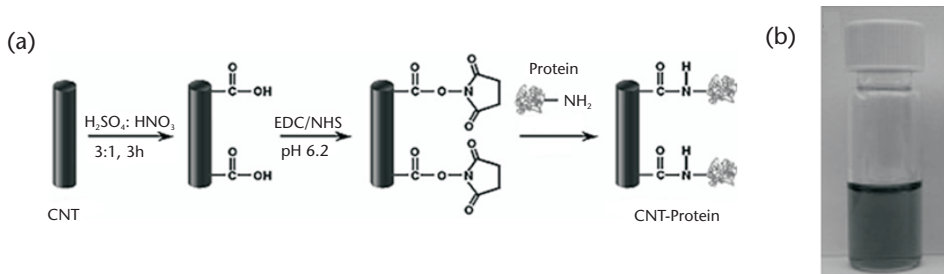


**Figure 1.2** CNT-protein composites. (a) Schematic of protein functionalization of carbon nanotubes. (b) Photograph of water-soluble MWNTs. (Adapted from Asuri et al. [22].)

adsorption is useful for studying the influence of the hydrophobic nanoscale environment of carbon nanotubes on protein structure and function. Also, enzyme activity measurement can be used to determine the stability of enzymes adsorbed onto nanotubes under harsh conditions.

#### 1.4.1.1 Measurement of Loading of Proteins on Carbon Nanotubes by the BCA Assay

The Pierce BCA Protein Assay uses a detergent-compatible formulation based on bicinchoninic acid (BCA) for the colorimetric detection and quantification of total protein. It involves the reduction of  $\text{Cu}^{2+}$  to  $\text{Cu}^{1+}$  ions by proteins to form a water soluble complex with BCA that strongly absorbs at 562 nm. Using this assay, the loading of proteins on carbon nanotubes is calculated as follows:

$$\text{Amount of protein loaded per mg SWNT} = C_i \cdot V_i - \sum_n C_j \cdot V_j \quad (1.1)$$

where,

$C_i$  = Initial concentration of protein before exposing it to SWNTs;

$V_i$  = Initial volume of protein solution added to SWNT dispersion;

$C_j$  = Concentration of supernatant in  $j$ th wash;

$V_j$  = Volume of supernatant in  $j$ th wash;

$n$  = Number of washes performed.

Representative data for the loading of SBP on SWNTs is shown in Figure 1.3(a). The adsorption of SBP followed a pseudosaturation behavior, with a maximum loading of  $575 \mu\text{g}$  SBP/mg SWNTs (Figure 1.3(a)). We observed that adsorbed SBP has a strong affinity for the SWNTs, with almost complete adsorption observed within the first minute (data not shown). Protein adsorption was irreversible at lower loadings. For example, at a loading of  $250\text{-}\mu\text{g}$  protein/mg SWNT, essentially no protein desorption was observed (Figure 1.3(b)). The AFM images of SWNT-SBP conjugates are shown in Figure 1.3(c) and (d). The globular structures seen on the wire like SWNTs represent SBP molecules. Line scans reveal that a region on the SWNTs that does not contain SBP has a height of 3.7 nm, while a region containing SBP has a height of 9.6 nm, the difference (5.9 nm) being the height of adsorbed SBP molecules.

#### 1.4.1.2 Retention of Protein Activity Upon Physical Adsorption

Adsorption onto CNTs can influence the structure, function, and stability of proteins. Since the catalytic activity of proteins relies on the retention of their native structure, measurement of catalytic activity can be used to evaluate the influence of the nanoscale environment of a CNT on protein properties. Using enzymes as highly sensitive probes of protein function, we studied the strong influence of the CNT surface on protein function and stability in harsh environments.

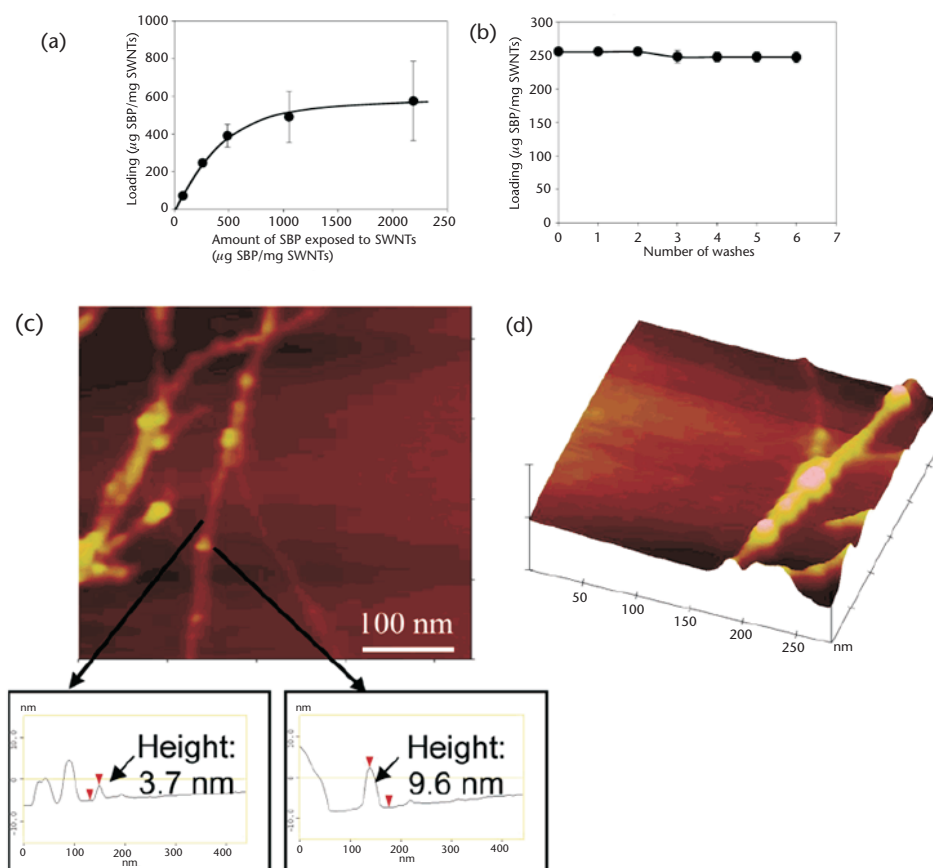


**Figure 1.3** Loading of SBP on SWNTs: (a) Protein loading as a function of amount of SBP exposed to SWNTs. (b) Protein loading as a function of washing with fresh buffer. (c) AFM images of SBP adsorbed onto SWNTs. (d) Surface plot of height image for SBP adsorbed onto SWNTs revealing SBP molecules on the SWNTs. (Reprinted with permission from Karajanagi et al. . Copyright (2004) American Chemical Society [7].)

#### Determination of Protein Activity Upon Physical Adsorption

The structure, function, and spatial orientation of proteins attached onto carbon nanotubes strongly depends on the interactions of the nanotube surface with proteins. Since the catalytic activity and exquisite selectivity of proteins requires the near complete retention of native structure, measurement of enzyme activity can be used to evaluate the influence of the hydrophobic nanoscale environment of nanotubes on enzyme structure and function. To that end, comparison of the activity of native and immobilized enzyme can provide insight into the influence of carbon nanotubes on the retention or loss of native-like enzyme properties.

As an example, the activity of native SBP was measured using *p*-cresol as the substrate [27]. SBP catalyzes the oxidation of *p*-cresol in the presence of  $\text{H}_2\text{O}_2$  to form fluorescent oligo- and polyphenol products. The initial reaction rates were measured by tracking the increase in fluorescence of the reaction mixture at excitation and emission wavelengths of 325 nm and 402 nm, respectively, using an HTS 7000 Plus Bio Assay Reader (Perkin-Elmer, Wellesley, MA). For a typical solution-phase assay, 0.15-µg/mL SBP was used with 20-mM *p*-cresol and 0.125-mM  $\text{H}_2\text{O}_2$  in a volume of 200 µL. To measure the

activity of SBP adsorbed onto SWNTs, a well-mixed dispersion of SWNT-SBP at a concentration of 1.0 mg/mL was prepared in aqueous buffer. For a typical experiment, 0.2–2.5  $\mu\text{g}$  of SWNTs were used on the basis of the loading of SBP. It was found that SBP retained significant specific activity at all loadings (Figure 1.4) ranging from 18 to 280  $\mu\text{g}$  SBP/ mg SWNTs. The specific activity of SBP was strongly dependent on the loading; up to 28% of native solution activity was obtained at 50% of maximal surface coverage, and this value dropped to ca. 10% at 3% of maximal surface coverage (Figure 1.4). The increase in specific activity of adsorbed SBP with an increase in the surface coverage on SWNTs may be due to a higher retention of native structure at higher surface loadings.

#### Protein Stability under Harsh Conditions

Physical adsorption of proteins to carbon nanotubes enhances the stability of proteins in strongly denaturing environments where native proteins undergo substantial deactivation. To determine protein stability at elevated temperatures (Figure 1.5(a)), the nanotube-protein conjugates were subjected to these temperature conditions for different periods of time and cooled in an ice bath. Initial enzymatic reaction rates were then determined at room temperature. To determine rate constants in approximately 100% methanol (Figure 1.5(b)), the initial rates were measured in methanol as a function of incubation time. The deactivation constant was determined from the slope of a straight-line fit through the plot of  $\log_e$  (% activity retained) versus time.

#### 1.4.1.3 Determination of Protein Secondary Structure Using Fourier Transform Infrared (FT-IR) Spectroscopy

FT-IR spectroscopy is an established tool for the structural characterization of proteins [29]. The secondary structure of a protein can be quantitatively determined from a spectrum by considering the amide I region, between 1,600 and 1,700  $\text{cm}^{-1}$ . This region, which consists mainly of the C-O stretching vibration of the backbone peptide bonds in proteins, was used to obtain the  $\alpha$  helix and  $\beta$  sheet contents of the protein [30, 31]. We

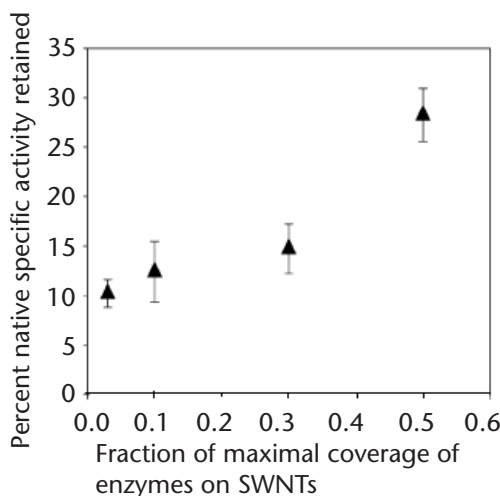


**Figure 1.4** Enzymatic activity retained as a function of the surface coverage of SBP adsorbed on SWNTs ( $\blacktriangle$ ). (Reprinted with permission from Karajanagi et al. [7]. Copyright (2004) American Chemical Society.)

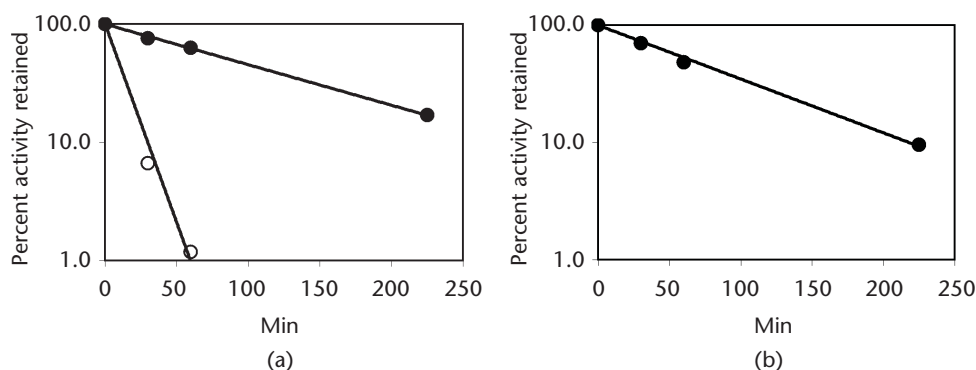


**Figure 1.5** Time-dependent deactivation of native SBP (○) and SBP on SWNTs (●) (a) at 95°C and (b) in 100% methanol. The activities are normalized relative to the initial activity (activity at  $t = 0$  min). Figure 1.5(b) does not contain % activity data for native SBP as it shows no activity in 100% methanol. (Reprinted with permission from Asuri et al. [28]. Copyright (2006) American Chemical Society.)

used FT-IR spectroscopy to compare the secondary structure of proteins before and after their adsorption onto carbon nanotubes. The differences in secondary structure between the soluble and adsorbed states are represented by the simple sum of magnitudes of changes in  $\alpha$  helix and  $\beta$  sheet contents. For example, SBP showed a total change in  $\alpha$  helical and  $\beta$  sheet content of 13% (Table 1.1), which suggests that SBP retains much of its native structure and activity upon absorption onto SWNTs.

#### 1.4.2 Characterization of Protein-Solubilized Carbon Nanotubes

The aggregation state of the protein solubilized carbon nanotube dispersions can be characterized by ultraviolet-visible (UV-Vis) and Raman spectroscopy. These methods can be used effectively to distinguish between solubilized and nonsolubilized carbon nanotubes. We describe the use of these two techniques to characterize the solubilized CNTs.

##### 1.4.2.1 Characterization of Carbon Nanotube Dispersions Using UV-Vis Spectroscopy

The UV-Vis absorption spectra of dispersions of SWNTs are known to be sensitive to their aggregation state [15]. The UV-Vis spectrum for SWNTs in water in the absence of a dispersing agent was essentially featureless, which indicates the presence of aggregates of SWNTs (data not shown). In contrast, the UV-Vis spectra for solutions of SWNTs

**Table 1.1** Secondary Structure Percentages of SBP in Solution and Adsorbed onto SWNTs, as Determined by FT-IR Spectroscopy Calculated from the Amide I Spectra

Sample	% $\alpha$ Helix	% $\beta$ Sheet
Native solution of SBP	36.1 $\pm$ 1.2	25.1 $\pm$ 2.5
SBP adsorbed onto SWNTs	27.9 $\pm$ 4.1	20.6 $\pm$ 6.9

(Adapted from Karajanagi et al. [7])



obtained using the proteins BSA and MJL exhibited sharp and well-resolved peaks (Figure 1.6). These sharp van Hove peaks are a characteristic of aqueous solutions containing debundled, individually dispersed SWNTs. The UV-Vis spectrum for SWNTs dispersed in water using NaDDBS also shows similar sharp features (Figure 1.6). We note that the spectra for SWNT-BSA and SWNT-MJL show peaks in the region beyond 900 nm that are red-shifted by approximately 10 to 15 nm with respect to those for SWNT-NaDDBS. This shift may be attributed to the greater accessibility of water to the SWNT surface for SWNT-BSA and SWNT-MJL than for SWNT-NaDDBS. It has been shown [32] that proteins can form a more porous layer on the SWNT surface than surfactants, thereby permitting water and other small molecules to associate with the surface.

#### 1.4.2.2 Raman Spectroscopy to Probe Aggregation State of SWNTs

Raman spectroscopy is a versatile tool, which enables us to probe the aggregation state of SWNTs in solutions. In the case of protein-solubilized SWNT dispersions, the radial breathing mode ( $150\text{--}350\text{ cm}^{-1}$ ) and tangential mode observations can be used as indicators of the quality of nanotube dispersion. To obtain the Raman spectra of the solubilized SWNT-BSA conjugates,  $10\text{ }\mu\text{g}$  of the conjugates were placed on a cleaned silicon substrate and samples were analyzed using a laser excitation at  $785\text{ nm}$  at a power of  $10\text{ mW}$ , with a  $50\times$  lens. (Spectra were recorded from  $0\text{--}3000\text{ cm}^{-1}$  for 4 minutes). The wavenumber calibration was carried out using the  $521\text{-cm}^{-1}$  line of silicon substrate as a reference. The relative intensities of Raman peaks in the region between  $230$  and  $270\text{ cm}^{-1}$  were found to be good indicators of the nanotube dispersion because of the change in Raman spectrum depending on their dispersed state. Specifically, in the aggregated state,  $(10,2)$  nanotubes are in resonance and  $(10,5)$  nanotubes are off resonance, while when SWNTs are dispersed,  $(10,5)$  nanotubes are in resonance and  $(10,2)$  nanotubes are off resonance. Accordingly, we see a peak at  $267\text{ cm}^{-1}$  for SWNT aggregates, whereas solubilized SWNT-BSA conjugates show no peak at  $267\text{ cm}^{-1}$  but a prominent peak at  $234\text{ cm}^{-1}$  (Figure 1.7(a)). Furthermore, the peak corresponding to the tangential mode (centered at  $1,591\text{ cm}^{-1}$ ) for soluble SWNT-BSA was narrower than that for the aggregated

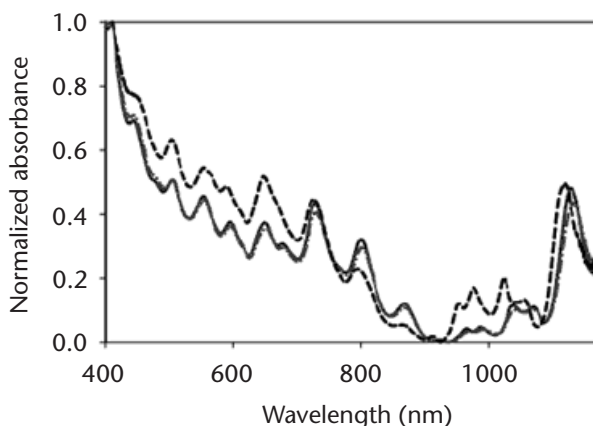


**Figure 1.6** UV-Vis absorption spectra of SWNTs dispersed in water using NaDDBS (dashed line), BSA (solid line), and MJL (dash-dot line) normalized at  $410\text{ nm}$ . (Reprinted with permission from Karajanagi et al. [14]. Copyright 2006 American Chemical Society.)

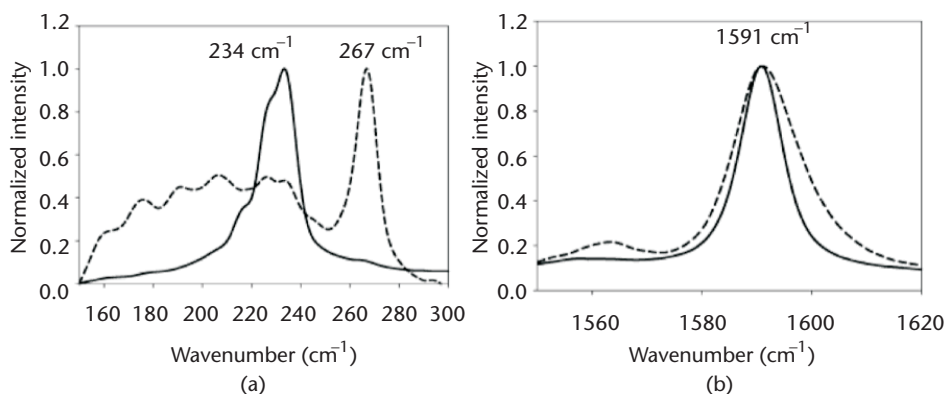


**Figure 1.7** Raman spectroscopic analysis of SWNT-BSA conjugates (solid line) and SWNTs (dashed line) in (a) Radial breathing mode, (b) Tangential mode at 785-nm excitation. (Reprinted with permission from Karajanagi et al. [14]. Copyright 2006 American Chemical Society.)

SWNTs, with a decrease in the full width at a half-maximum of approximately  $5\text{ cm}^{-1}$  (Figure 1.7(b)), which is in agreement with similar observations for solutions containing individually dispersed SWNTs [20, 33, 34].

### 1.4.3 Characterization of Covalently Attached Carbon Nanotube-Protein Conjugates

We determined the retention of protein structure and function upon covalent attachment to carbon nanotubes using Hammett analysis of protein activity as well as spectroscopic techniques, such as CD and fluorescence spectroscopies. Structural analysis by CD or fluorescence spectroscopy is not possible for conjugates prepared by physical adsorption of proteins onto bundles of nanotubes or for covalent MWNT-protein conjugates because of interference from the carbon nanotubes. On the other hand, because of the higher solubility and higher protein loading obtained in case of covalent attachment of proteins to oxidized SWNTs, CD, and fluorescence measurement-based structural studies are possible. The activity measurements of the nanotube-protein conjugates indicated that the conjugates demonstrated not only enhanced stability in harsh conditions, but also operational and storage stability.

#### 1.4.3.1 Hammett Analysis for Protein Structure-Activity Relationship

It is often important to study the structural perturbations of the protein to further probe the effects of immobilization. However, analyses of proteins on MWNTs, such as CD and FT-IR spectroscopy, are hindered by the strong absorbance and intrinsic fluorescence of nanotubes. Hammett analysis, on the other hand, is a well-established kinetic technique to probe an enzyme's transition state structure [27]. In the case of SBP catalysis, the Hammett coefficient  $\rho$  provides a measure of the sensitivity of SBP's catalytic efficiency to the electronic nature of substituents on phenolic substrates (electron-donating or electron-withdrawing), as reflected in the values of their substituent electronic parameter  $\sigma$ . Positive values of  $\sigma$  represent electron withdrawal by the substituent from the aromatic ring, whereas negative values indicate electron release to the ring. Deviation in  $\rho$  values for SBP bound to a support from that for the native enzyme in aqueous buffer

would indicate that the active site structure of the enzyme is perturbed by adsorption onto the support.

$$\log\left(\frac{V_{max}}{K_M}\right) = \sigma \cdot \rho + constant \quad (1.2)$$

To that end, we determined the Hammett coefficient,  $\rho$ , based on a modified form of the Hammett equation for SBP (1.2), using a series of phenolic substrates,  $p$ -OC<sub>2</sub>H<sub>5</sub>,  $p$ -CH<sub>3</sub>,  $p$ -CH<sub>2</sub>OH, and  $p$ -Cl with different values of the electronic parameter ( $\sigma$ ) varying from -0.24 to +0.23 [27].<sup>1</sup> The standard kinetic parameters—maximum reaction rate ( $V_{max}$ ) and Michaelis constant ( $K_M$ )—were determined for the different substrates using nonlinear Michaelis-Menten fits. Figure 1.8 depicts the Hammett analysis for native SBP and MWNT-SBP in aqueous buffer. Interestingly, the Hammett coefficients for native and immobilized SBP are essentially identical. The comparable values of  $\rho$  indicate that the differences in the active site structure for native and immobilized SBP are minimal; therefore, the mechanism of catalysis for MWNT-SBP is similar to that for native SBP. Thus, the high retention of catalytic activity for the MWNT-SBP conjugates is consistent with the enzyme retaining its intrinsic active site structure throughout the attachment process.

#### 1.4.3.2 Determination of Protein Secondary Structure Using Circular Dichroism (CD) Spectroscopy

CD spectroscopy is used for studying the conformational stability of a protein under harsh conditions—thermal stability, pH stability, and stability against chemical denaturants. CD measures the difference in absorbance of a sample between left-hand polarized light and right-hand polarized light; these differences arise because of

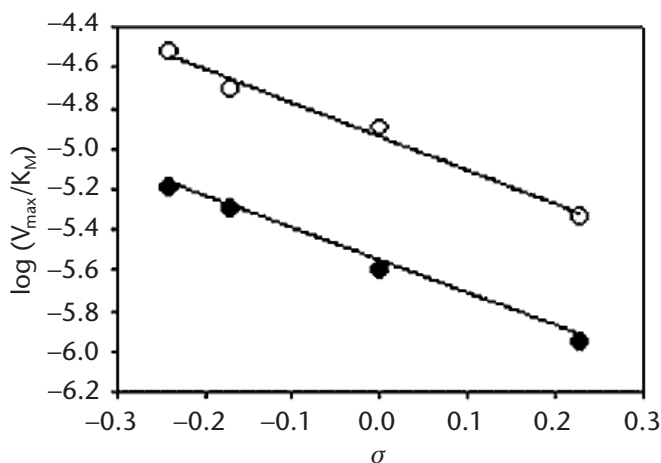


**Figure 1.8** Influence of the substituent electronic parameter,  $\sigma$ , on the catalytic efficiency of native SBP (○) and MWNT-SBP conjugates (●) in aqueous buffer. Slope of the lines gives the Hammett coefficient in each case:  $\rho$  for native SBP =  $-1.6 \pm 0.1$ ;  $\rho$  for MWNT-SBP =  $-1.5 \pm 0.2$ . (Adapted from Asuri et al. [22].)

<sup>1</sup> The values of the electronic parameter ( $\sigma$ ) for  $p$ -OC<sub>2</sub>H<sub>5</sub>,  $p$ -CH<sub>3</sub>,  $p$ -CH<sub>2</sub>OH, and  $p$ -Cl are -0.24, -0.17, 0.00, and 0.23 respectively.

structural asymmetry in a molecule. Secondary protein structure is usually comprised of  $\alpha$  helices and  $\beta$  sheets, each producing a characteristic spectrum in the far-UV range (190–250 nm).  $\alpha$  helices produce a spectrum with valleys around 208 and 222 nm, while  $\beta$  sheets show a single valley around 215 nm. As proteins lose their native structure and become less ordered, the absence of regular structure is reflected in zero CD intensity. Thus, by measuring the far-UV CD spectrum of a protein before and after attachment onto nanotubes, one can get an idea of how the structure of the protein has been altered. Using data processing software that can analyze a CD spectrum and determine the relative content of  $\alpha$  helix and  $\beta$  sheet, we determined that HRP attached to SWNTs retained 68% of its native  $\alpha$  helix content (Figure 1.9).

We used CD spectroscopy to monitor the change in the secondary structure of HRP upon exposure to varying concentrations of GdnHCl denaturant and high temperatures. The secondary structure of HRP and SWNT-HRP conjugates were thus monitored by CD, using a protein concentration of 0.05 mg/mL, in the presence or absence of denaturant. After equilibrating the samples with GdnHCl for 24 hours, CD spectra were measured (Figure 1.10(b)). The concentration of GdnHCl required to denature the protein by 50% in the sample ( $C_m$ ) increased from 1.6 to 2.4M as a result of conjugation. For thermal denaturation, the temperature was slowly raised (0.5°C/min) from 20°C to 99°C while spectra were taken (Figure 1.10(a)). The temperature required to unfold the protein by 50% in the sample ( $T_m$ ) increased from 79°C to 92°C for the SWNT-HRP conjugate. Characterization by CD spectroscopy therefore revealed a substantial increase in protein stability under stronger denaturing conditions and higher temperatures when covalently attached to SWNTs.

#### 1.4.3.3 Characterization of Protein Tertiary Structure Using Tryptophan Fluorescence

Proteins contain three aromatic amino acid residues (tryptophan, tyrosine, and phenylalanine), which contribute to their intrinsic fluorescence. In particular, the polarity and charge densities surrounding tryptophan residues influence both the fluorescence intensity and maximal emission fluorescence wavelength ( $\lambda_{max}$ ). As the protein denatures, losing its tertiary structure, the environment around buried tryptophan resi-

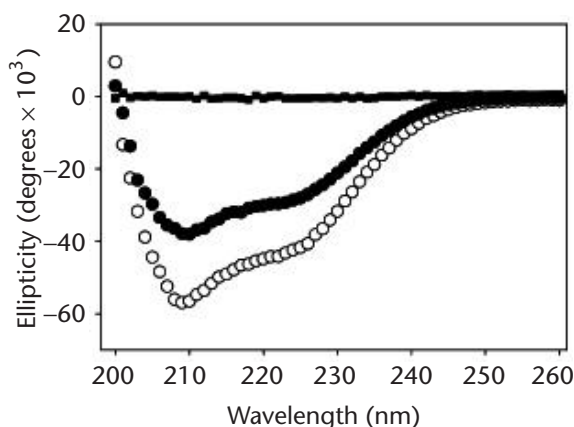


**Figure 1.9** Far-UV CD spectra of native HRP (○), SWNT-HRP (●), and bare SWNTs (■). (Reprinted with permission from Asuri et al. [35]. Copyright 2007 American Chemical Society.)

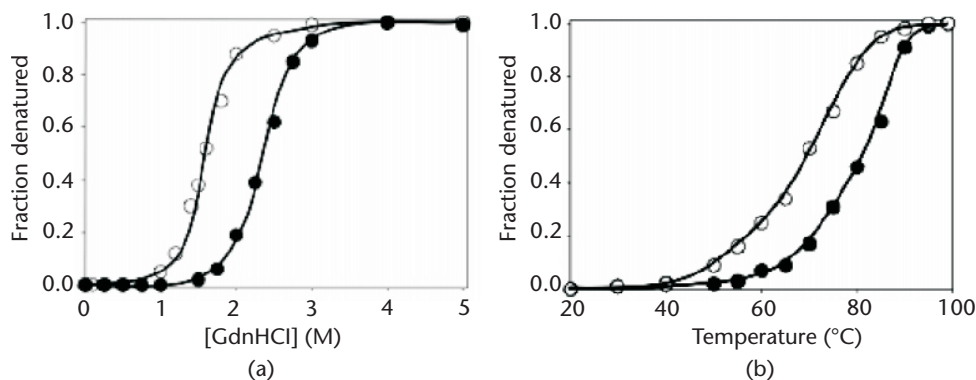


**Figure 1.10** Fraction of HRP denatured determined by monitoring the CD signal at 222 nm of native HRP (○) and SWNT-HRP (●) as a function of (a) GdnHCl concentration and (b) solution temperature. (Reprinted with permission from Asuri et al. [35]. Copyright 2007 American Chemical Society.)

dues changes drastically, eventually leading to their exposure to solution. Thus, upon protein denaturation, the fluorescence intensities and tryptophan emission wavelength tend toward those of free tryptophan in solution; structural changes can thus be inferred from alteration of the tryptophan's microenvironment.

As an example, the protein HRP contains one buried tryptophan residue at position 117 [36]. When GdnHCl was used as the denaturant (Figure 1.11), the fluorescence intensities and  $\lambda_{\max}$  values for both native HRP and SWNT-HRP conjugate were lower than those for free L-tryptophanamide when excited at 283 nm at lower Gdn HCl concentrations [27, 36]; however, at higher GdnHCl concentrations, both the values approached those of L-tryptophanamide, indicating that HRP's tryptophan residue was now more accessible to the solvent due to protein denaturation. The SWNT-HRP conjugates showed a more gradual increase toward the values of L-tryptophanamide than native HRP, indicating that they are more stable under denaturing conditions than native HRP.

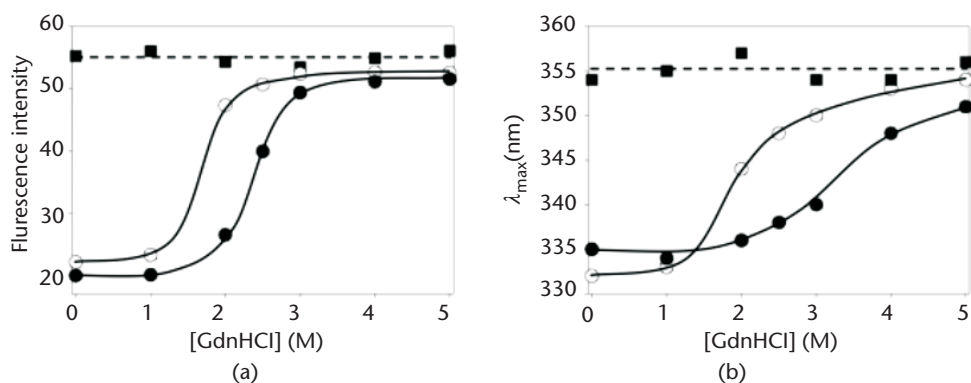


**Figure 1.11** (a) Fluorescence intensity (excitation at 283 nm and emission at  $\lambda_{\max}$ ) and (b)  $\lambda_{\max}$  of L-tryptophanamide (■), native HRP (○), and SWNT-HRP (●) as a function of GdnHCl concentration. (Reprinted with permission from Asuri et al. [35]. Copyright 2007 American Chemical Society.)

#### 1.4.3.4 Thermostabilization of Proteins Via Covalent Attachment onto Carbon Nanotubes

Exposure of proteins to high temperatures can lead to irreversible unfolding and deactivation, posing a critical limitation to their commercial use. We have found that covalent attachment of proteins onto MWNTs leads to thermostabilization of the protein. There is a certain optimal temperature ( $T_{opt}$ ) at which the protein's catalytic activity is at its maximum, beyond which the protein unfolds and gets deactivated irreversibly. The thermostabilization of proteins upon immobilization causes an elevation in  $T_{opt}$  values. While the  $T_{opt}$  for native SBP was found to be approximately 75°C, the MWNT-SBP conjugates displayed a  $T_{opt}$  of approximately 90°C (Figure 1.12), which is close to the native melting temperature of SBP ( $T_m = 90.5^\circ\text{C}$ ) [37]. This enhanced stability of MWNT-SBP leads to a 2.5-fold increase in the maximal initial reaction rate at 90°C as compared to that of native SBP at 75°C, thus rendering the protein formulation well suited for applications where harsh conditions are required.

#### 1.4.3.5 Operational and Storage Stability of Carbon Nanotube-Enzyme Conjugates

Two other issues concerning the commercial use of native enzymes in biocatalysis are difficulty of enzyme reuse and loss of enzymatic activity on prolonged storage. While macroscopic supports provide ease of separation and reusability of immobilized enzymes, stabilization provided by such supports is significantly less compared to nanoscale supports [28]. On the other hand, use of inherently long oxidized MWNTs for attaching enzymes not only stabilizes enzymes under different reaction and storage conditions but also allows easy recovery of conjugates from reaction mixture through filtration. A mat-like film forms after filtering the reaction mixture through the filter membrane; this film can be redispersed in an aqueous buffer by minimal sonication. For example, SBP, which was covalently attached to MWNT, retained about 70% of its initial activity even after being reused over 100 times (Figure 1.13(a)). Additionally, such conjugates were found to be stable for an extended period. Even after 30 days, the MWNT-SBP conjugates retained ca. 70% of their initial activity (Figure 1.13(b)). On the other hand, native SBP retained only about 30% of its initial activity. These observations indeed suggest that

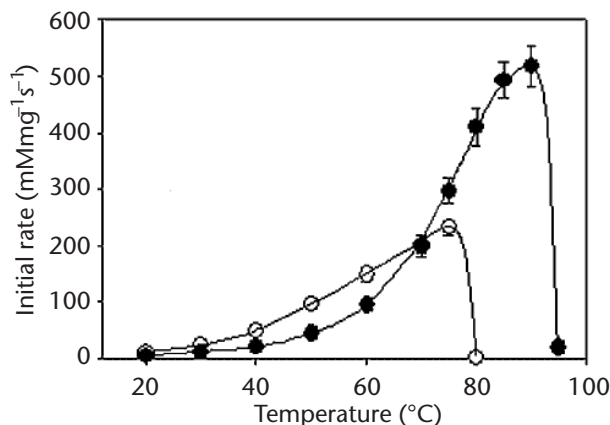


**Figure 1.12** Influence of temperature on the kinetics of native SBP (○) and MWNT-SBP (●) in aqueous buffer. (Adapted from Asuri et al. [22].)

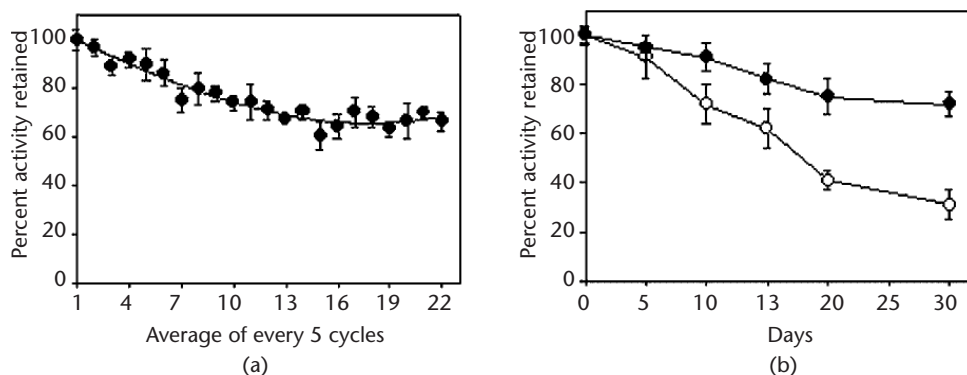


**Figure 1.13** Operational and storage stability of MWNT-SBP. (a) Reusability of MWNT-SBP conjugates. (b) Retention of enzymatic activity in aqueous buffer at room temperature—native SBP (○) and MWNT-SBP (●). (Adapted from Asuri et al. [22].)

nanoscale supports, such as MWNTs, make the enzyme formulation reusable and storage compatible.

## 1.5 Discussion and Commentary

As discussed in the previous sections, characterization of CNT-protein conjugates exhibits the subtle differences observed due to these different methods of protein immobilization on CNTs. Biofunctionalization of CNTs and characterization of resultant hybrid material has been carried out for various reasons. First, it is of great interest to study how different biomolecules interact with carbon nanotubes compared to conventional micro or macroscale supports. For this study, biomolecules were interfaced with nanotubes through physical adsorption or covalent attachment. Second, use of CNTs, as drug delivery vehicles or for construction of self-assembled nanoscaled superstructures, requires them to be water soluble. The amphiphilic nature of biomolecules can be exploited in solubilizing CNTs. Additionally, these biofunctionalized CNTs can be used in a wide range of applications, which include biosensing, bioelectrochemistry, biomedicine, and intracellular delivery of peptides and proteins. In the course of preparing such nanobiocomposite materials and realizing their potential applications, we have critically optimized our protocols to overcome some of the problems that can occur with these techniques. In this section, we discuss some precautions to take while preparing nanotube-protein conjugates.

CNTs, being in the form of clumpy or fluffy black powder, should be handled using personal protective equipment and in safety hoods with adequate ventilation. If inhaled, remove to fresh air. If breathing difficulties persist, get medical attention. In case of contact, immediately flush eyes or skin with plenty of water for at least 15 minutes. If irritation develops or persists, get medical attention. During physical adsorption of proteins, we have observed that protein adsorption occurs in the initial 5 to 10 minutes of mixing CNTs and protein solutions. Therefore, before mixing these solutions, it is necessary to achieve a uniform dispersion of CNTs through effective sonication. As an additional precaution, it is advisable to thaw the protein-containing vial after removing

it from storage temperature of 4°C or –20°C. This is to ensure that the protein powder does not pick up unwanted moisture on exposure to air.

As a common safety practice, it is recommended to handle acids in fume hoods while carrying out acid oxidation of CNTs. During the sonication step, intermittent swirling of nanotube-acid mixture would maintain well-mixed reaction conditions. The rise in temperature due to exothermic acid oxidation and sonication leads to heating up of water bath, which could cause excessive oxidation of CNTs and hence formation of fine, non-recoverable particles. Therefore, periodic replacement of water in the bath with ice-cold water is necessary for maintaining desired operating conditions. Filtration of CNTs after acid oxidation leads to formation of a densely packed nanotube mat. A simplistic approach to get uniform nanotube suspension would be to disperse this nanotube film in enough volumes of milliQ water by sonication. After ester functionalization and filtration of oxidized CNTs, ensure that the filtered CNTs film does not dry out completely; disperse the film immediately in protein solution. The pH of the buffer used for carrying out EDC-NHS chemistry was found to govern the extent of ester functionalization onto carbon nanotubes. While a pH range of 4 to 7 is suitable, lower pH conditions results in higher functionalization and hence higher protein attachment.

There are a few notable differences between the three methods of nanotube-protein preparation, and the choice of one over the other is governed by the properties of conjugates desired and their end application. Some of the differences between physical adsorption of proteins onto CNTs, protein solubilization of CNTs, and covalent attachment methods of proteins onto CNTs are listed in Table 1.2.

### Troubleshooting Table

Problem	Explanation	Potential Solution
Low catalytic activity of proteins upon covalent attachment.	Low protein attachment onto oxidized CNTs in EDC-NHS reaction steps.	Prolonged exposure of active ester to air can lead to its hydrolysis. Add protein solution immediately after nanotube activation.
Presence of CNT aggregates after acid oxidation and filtration steps.	Inefficient oxidation of CNTs.	Increase acid treatment duration.

## 1.6 Applications Notes

The methods of noncovalent and covalent functionalization of carbon nanotubes with proteins have been used in numerous applications two of which are highlighted in this

**Table 1.2** General Comparison Between the Three Methods of Protein Attachment onto CNTs

Physical Adsorption of Proteins onto CNTs	Protein Solubilization of CNTs	Covalent Attachment of Proteins onto CNTs
Ease of attachment	Ease of attachment	Cumbersome with many steps involved
Facile method of attachment preserves native structural and functional properties of both CNTs and proteins	Ultrasonication can lead to protein denaturation	Chemical modification of CNTs can compromise its native electronic and mechanical properties
Leaching of proteins upon agitation and storage	Leaching of proteins upon agitation and storage	No leaching effect observed
Conjugates present in aggregate form	Conjugates are water-soluble	Conjugates are water-soluble
Conjugates can be separated from solution by centrifugation	Conjugates can be separated from solution by filtration	Conjugates can be separated from solution by filtration



section. As our first example, we consider the role of nanobiocomposites in carrying out biotransformation in biphasic medium wherein phase transfer biocatalysis involves the mass transfer of water-insoluble substrates from organic to aqueous phase. Therefore, interfacial adsorption of enzymes is desired to carry out biotransformations at the aqueous-organic interface. We have demonstrated that SWNTs along with the attached protein can be directed to aqueous-organic interfaces with the aid of surfactants [38]. SWNTs as a protein support not only provide high intrinsic surface area but also overcome any intraparticle diffusional limitations that restrict use of enzymes in biphasic system. We showed that physical adsorption increased specific enzyme activity by three orders of magnitude as compared to native enzymes in aqueous phase, with enhanced stability at high temperatures. Thus, the nanotube-mediated interfacial assembly of enzymes can be very advantageous in directing greater amounts of enzymes from the bulk aqueous phase to the interface and in increasing the stability of enzymes against inactivation.

The procedure of covalent attachment of proteins onto carbon nanotubes has been successfully employed to produce highly active and stable DNAzyme-carbon nanotube hybrids. Certain small single-stranded DNA fragments possess catalytic activity (e.g., endonuclease-type activity) and are known as DNAzymes [39]. Yim et al. covalently attached streptavidin to acid-treated MWNTs using EDC-NHS chemistry, followed by the binding of biotinylated DNAzyme to yield MWNT-DNAzyme conjugates that were soluble in aqueous buffer [40]. The MWNT-DNAzyme conjugates followed Michaelis-Menten kinetics under the conditions where substrate concentration is higher than that of DNAzyme (Figure 1.14). Additionally, this hybridization led to a formulation providing very high turnover numbers, without the need for substrate-DNAzyme hybridization between each catalytic event. Conjugating such DNAzymes with nanomaterials can be of potential use in the development of biosensors to detect metal ions and nucleic acids as well as in designing strategies for directing nanoparticle assembly [41, 42].

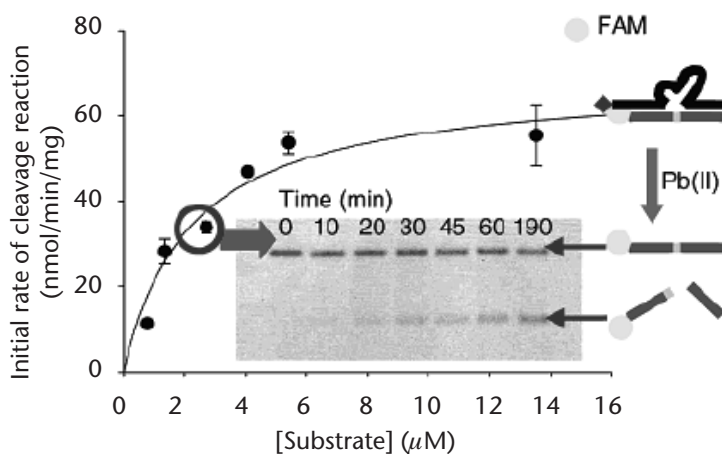


**Figure 1.14** Catalytic activity of MWNT-DNAzyme conjugates. The line represents a nonlinear fit of the Michaelis-Menten expression to the data. Inset shows analysis of extent of conversion of fluorescently labeled substrate DNA by polyacrylamide gel electrophoresis (PAGE), with upper band representing uncleaved DNA and lower band representing cleaved fragments. (Reprinted with permission from Yim et al. [40]. Copyright 2005 American Chemical Society.)

## 1.7 Summary Points

Physical adsorption of proteins onto CNTs is a simple and effective method for preparing nanotube-protein conjugates without any modification of electronic and mechanical properties of CNTs.

Protein assisted solubilization of CNTs can be important for biomedical applications, such as biomedical devices, cellular delivery; besides, the wide variety of functional groups on adsorbed proteins can act as orthogonal reactive handles for the functionalization of CNTs.

Water-soluble CNT-protein conjugates, prepared by acid oxidation of CNTs and covalent attachment of proteins, possess high enzyme activity, high stability and reusability, and low diffusional resistance; these conjugates can find application in biomaterials, biotransformations, medicine and self-assembled materials.

## Acknowledgments

The methods presented here would not have been possible without the dedicated work of Dr. Sandeep S. Karajanagi, Dr. Tae-Jin Yim, and Dr. Dae-Yun Kim who took part in the original investigations. We also thank Dr. Cerasela Zoica Dinu and Dr. Guangyu Zhu for insightful discussions and comments.

## References

- [1] Ajayan, P. M., "Nanotubes from carbon," *Chemical Reviews* Vol. 99, No. 7 1999, pp. 1787–1799.
- [2] Chen, R. J., Bangsaruntip, S., Drouvalakis, K. A., Kam, N. W. S., Shim, M., Li, Y. M., Kim, W., Utz, P. J., and Dai, H. J., "Noncovalent functionalization of carbon nanotubes for highly specific electronic biosensors," *Proceedings of the National Academy of Sciences of the United States of America* Vol. 100, No. 9 2003, pp. 4984–4989.
- [3] Pantarotto, D., Briand, J. P., Prato, M., and Bianco, A., "Translocation of bioactive peptides across cell membranes by carbon nanotubes," *Chemical Communications*, No. 1 2004, pp. 16–17.
- [4] Kam, N. W. S., Jessop, T. C., Wender, P. A., and Dai, H. J., "Nanotube molecular transporters: Internalization of carbon nanotube-protein conjugates into mammalian cells," *Journal of the American Chemical Society* Vol. 126, No. 22 2004, pp. 6850–6851.
- [5] Barone, P. W., Parker, R. S., and Strano, M. S., "In vivo fluorescence detection of glucose using a single-walled carbon nanotube optical sensor: Design, fluorophore properties, advantages, and disadvantages," *Analytical Chemistry* Vol. 77, No. 23 2005, pp. 7556–7562.
- [6] Kam, N. W. S., O'Connell, M., Wisdom, J. A., and Dai, H. J., "Carbon nanotubes as multifunctional biological transporters and near-infrared agents for selective cancer cell destruction," *Proceedings of the National Academy of Sciences of the United States of America* Vol. 102, No. 33 2005, pp. 11600–11605.
- [7] Karajanagi, S. S., Vertegel, A. A., Kane, R. S., and Dordick, J. S., "Structure and function of enzymes adsorbed onto single-walled carbon nanotubes," *Langmuir* Vol. 20, No. 26 2004, pp. 11594–11599. The authors investigate the structure and function of proteins immobilized onto SWNTs to develop a better understanding of SWNT-protein interactions.
- [8] Panhuis, M. I. H., Salvador-Morales, C., Franklin, E., Chambers, G., Fonseca, A., Nagy, J. B., Blau, W. J., and Minett, A. I., "Characterization of an interaction between functionalized carbon nanotubes and an enzyme," *Journal of Nanoscience and Nanotechnology* Vol. 3, No. 3 2003, pp. 209–213.
- [9] Carrillo, A., Swartz, J. A., Gamba, J. M., Kane, R. S., Chakrapani, N., Wei, B. Q., and Ajayan, P. M., "Noncovalent functionalization of graphite and carbon nanotubes with polymer multilayers and gold nanoparticles," *Nano Letters* Vol. 3, No. 10 2003, pp. 1437–1440.
- [10] Shim, M., Kam, N. W. S., Chen, R. J., Li, Y. M., and Dai, H. J., "Functionalization of carbon nanotubes for biocompatibility and biomolecular recognition," *Nano Letters* Vol. 2, No. 4 2002, pp. 285–288.

- [11] Pompeo, F., and Resasco, D. E., "Water solubilization of single-walled carbon nanotubes by functionalization with glucosamine," *Nano Letters* Vol. 2, No. 4 2002, pp. 369–373.
- [12] Star, A., Steuerman, D. W., Heath, J. R., and Stoddart, J. F., "Starched carbon nanotubes," *Angewandte Chemie-International Edition* Vol. 41, No. 14 2002, pp. 2508.
- [13] Asuri, P., Karajanagi, S. S., Kane, R. S., and Dordick, J. S., "Polymer-nanotube-enzyme composites as active antifouling films," *Small* Vol. 3, No. 1 2007, pp. 50–53.
- [14] Karajanagi, S. S., Yang, H. C., Asuri, P., Sellitto, E., Dordick, J. S., and Kane, R. S., "Protein-assisted solubilization of single-walled carbon nanotubes," *Langmuir* Vol. 22, No. 4 2006, pp. 1392–1395. The authors report a simple method that uses proteins to solubilize SWNTs in water.
- [15] O'Connell, M. J., Bachilo, S. M., Huffman, C. B., Moore, V. C., Strano, M. S., Haroz, E. H., Rialon, K. L., Boul, P. J., Noon, W. H., Kittrell, C., Ma, J. P., Hauge, R. H., Weisman, R. B., and Smalley, R. E., "Band gap fluorescence from individual single-walled carbon nanotubes," *Science* Vol. 297, No. 5581 2002, pp. 593–596.
- [16] Islam, M. F., Rojas, E., Bergey, D. M., Johnson, A. T., and Yodh, A. G., "High weight fraction surfactant solubilization of single-wall carbon nanotubes in water," *Nano Letters* Vol. 3, No. 2 2003, pp. 269–273.
- [17] O'Connell, M. J., Boul, P., Ericson, L. M., Huffman, C., Wang, Y. H., Haroz, E., Kuper, C., Tour, J., Ausman, K. D., and Smalley, R. E., "Reversible water-solubilization of single-walled carbon nanotubes by polymer wrapping," *Chemical Physics Letters* Vol. 342, No. 3–4 2001, pp. 265–271.
- [18] Huang, W. J., Fernando, S., Allard, L. F., and Sun, Y. P., "Solubilization of single-walled carbon nanotubes with diamine-terminated oligomeric poly(ethylene glycol) in different functionalization reactions," *Nano Letters* Vol. 3, No. 4 2003, pp. 565–568.
- [19] Zheng, M., Jagota, A., Semke, E. D., Diner, B. A., McLean, R. S., Lustig, S. R., Richardson, R. E., and Tassi, N. G., "DNA-assisted dispersion and separation of carbon nanotubes," *Nature Materials* Vol. 2, No. 5 2003, pp. 338–342.
- [20] Dieckmann, G. R., Dalton, A. B., Johnson, P. A., Razal, J., Chen, J., Giordano, G. M., Munoz, E., Musselman, I. H., Baughman, R. H., and Draper, R. K., "Controlled assembly of carbon nanotubes by designed amphiphilic peptide helices," *Journal of the American Chemical Society* Vol. 125, No. 7 2003, pp. 1770–1777.
- [21] Numata, M., Asai, M., Kaneko, K., Bae, A. H., Hasegawa, T., Sakurai, K., and Shinkai, S., "Inclusion of cut and as-grown single-walled carbon nanotubes in the helical superstructure of schizophyllan and curdlan (ss-1,3-glucans)," *Journal of the American Chemical Society* Vol. 127, No. 16 2005, pp. 5875–5884.
- [22] Asuri, P., Karajanagi, S. S., Sellitto, E., Kim, D. Y., Kane, R. S., and Dordick, J. S., "Water-soluble carbon nanotube-enzyme conjugates as functional biocatalytic formulations," *Biotechnology and Bioengineering* Vol. 95, No. 5 2006, pp. 804–811. The authors present a method of preparing water-soluble carbon nanotube-enzyme conjugates, which retain high activity and are stable at high temperatures.
- [23] Jiang, K. Y., Schadler, L. S., Siegel, R. W., Zhang, X. J., Zhang, H. F., and Terrones, M., "Protein immobilization on carbon nanotubes via a two-step process of diimide-activated amidation," *Journal of Materials Chemistry* Vol. 14, No. 1 2004, pp. 37–39.
- [24] Vix-Guterl, C., Couzi, M., Dentzer, J., Trinquocoste, M., and Delhaes, P., "Surface characterizations of carbon multiwall nanotubes: Comparison between surface active sites and Raman Spectroscopy," *Journal of Physical Chemistry B* Vol. 108, No. 50 2004, pp. 19361–19367.
- [25] Wang, P., "Nanoscale biocatalyst systems," *Current Opinion in Biotechnology* Vol. 17, No. 6 2006, pp. 574–579.
- [26] Huang, W. J., Taylor, S., Fu, K. F., Lin, Y., Zhang, D. H., Hanks, T. W., Rao, A. M., and Sun, Y. P., "Attaching proteins to carbon nanotubes via diimide-activated amidation," *Nano Letters* Vol. 2, No. 4 2002, pp. 311–314.
- [27] Ryu, K., and Dordick, J. S., "How Do Organic-Solvents Affect Peroxidase Structure and Function," *Biochemistry* Vol. 31, No. 9 1992, pp. 2588–2598.
- [28] Asuri, P., Karajanagi, S. S., Yang, H. C., Yim, T. J., Kane, R. S., and Dordick, J. S., "Increasing protein stability through control of the nanoscale environment," *Langmuir* Vol. 22, No. 13 2006, pp. 5833–5836. The authors report that carbon nanotubes may be used to enhance protein stability in harsh environments.
- [29] Jackson, M., and Mantsch, H. H., "The use and misuse of FTIR Spectroscopy in the determination of protein-structure," *Critical Reviews in Biochemistry and Molecular Biology* Vol. 30, No. 2 1995, pp. 95–120.
- [30] Dong, A., Huang, P., and Caughey, W. S., "Protein secondary structures in water from 2nd-derivative amide-I infrared spectra," *Biochemistry* Vol. 29, No. 13 1990, pp. 3303–3308.

- [31] Vedantham, G., Sparks, H. G., Sane, S. U., Tzannis, S., and Przybycien, T. M., "A holistic approach for protein secondary structure estimation from infrared spectra in H<sub>2</sub>O solutions," *Analytical Biochemistry* Vol. 285, No. 1 2000, pp. 33–49.
- [32] Barone, P. W., Baik, S., Heller, D. A., and Strano, M. S., "Near-infrared optical sensors based on single-walled carbon nanotubes," *Nature Materials* Vol. 4, No. 1 2005, pp. 86–U16.
- [33] Dalton, A. B., Stephan, C., Coleman, J. N., McCarthy, B., Ajayan, P. M., Lefrant, S., Bernier, P., Blau, W. J., and Byrne, H. J., "Selective interaction of a semiconjugated organic polymer with single-wall nanotubes," *Journal of Physical Chemistry B* Vol. 104, No. 43 2000, pp. 10012–10016.
- [34] Rao, A. M., Chen, J., Richter, E., Schlecht, U., Eklund, P. C., Haddon, R. C., Venkateswaran, U. D., Kwon, Y. K., and Tomanek, D., "Effect of van der Waals interactions on the Raman modes in single walled carbon nanotubes," *Physical Review Letters* Vol. 86, No. 17 2001, pp. 3895–3898.
- [35] Asuri, P., Bale, S. S., Pangule, R. C., Shah, D. A., Kane, R. S., and Dordick, J. S., "Structure, function, and stability of enzymes covalently attached to single-walled carbon nanotubes," *Langmuir* Vol. 23, No. 24 2007, pp. 12318–12321.
- The authors report that enzymes covalently attached to SWNTs retain a high fraction of their native structure and function, with enhanced stability in harsh environments.
- [36] Welinder, K. G., "Amino-Acid Sequence Studies of Horseradish-Peroxidase .4. Amino and Carboxyl Termini, Cyanogen-Bromide and Tryptic Fragments, the Complete Sequence, and Some Structural Characteristics of Horseradish Peroxidase-C," *European Journal of Biochemistry* Vol. 96, No. 3 1979, pp. 483–502.
- [37] McEldoon, J. P., and Dordick, J. S., "Unusual thermal stability of soybean peroxidase," *Biotechnology Progress* Vol. 12, No. 4 1996, pp. 555–558.
- [38] Asuri, P., Karajanagi, S. S., Dordick, J. S., and Kane, R. S., "Directed assembly of carbon nanotubes at liquid-liquid interfaces: Nanoscale conveyors for interfacial biocatalysis," *Journal of the American Chemical Society* Vol. 128, No. 4 2006, pp. 1046–1047.
- The authors demonstrate that SWNT-enzyme conjugates can be directed to aqueous-organic interfaces and used for interfacial biocatalysis.
- [39] Li, Y. F., and Breaker, R. R., "Deoxyribozymes: new players in the ancient game of biocatalysis," *Current Opinion in Structural Biology* Vol. 9, No. 3 1999, pp. 315–323.
- [40] Yim, T. J., Liu, J. W., Lu, Y., Kane, R. S., and Dordick, J. S., "Highly active and stable DNAzyme - Carbon nanotube hybrids," *Journal of the American Chemical Society* Vol. 127, No. 35 2005, pp. 12200–12201.
- [41] Liu, J. W., and Lu, Y., "A colorimetric lead biosensor using DNAzyme-directed assembly of gold nanoparticles," *Journal of the American Chemical Society* Vol. 125, No. 22 2003, pp. 6642–6643.
- [42] Sando, S., Sasaki, T., Kanatani, K., and Aoyama, Y., "Amplified nucleic acid sensing using programmed self-cleaving DNAzyme," *Journal of the American Chemical Society* Vol. 125, No. 51 2003, pp. 15720–15721.